International Journal of Control and Automation
Vol. 8, No. 6 (2015), pp. 121-138
http://dx.doi.org/10.14257/ijca.2015.8.6.13

A Low Frequency Vibration Control by Synchronized Switching on Negative Capacitance and Voltage Sources

Ehtesham Mustafa Qureshi [1], Xing Shen[a, b], and Lulu Chang[a]

[a] *College of Aerospace Engineering, State Key Laboratory of Mechanics and Control of Mechanical Structures, Nanjing University of Aeronautics and Astronautics, No. 29 Yudao Street, Nanjing 210016, China*
ehteshammustafa@gmail.com; [b]shenx@nuaa.edu.cn (corresponding author); luluchang@nuaa.edu.cn

Abstract

Synchronized switch damping (SSD) techniques have recently been developed, as an alternative to active vibration control techniques, to address the problem of structure vibration control. In these techniques, a piezoelectric patch is bonded on the vibrating structure and shunted by a network of electrical elements. During the structure motion, the piezoelectric patch is connected and disconnected from the shunt circuit, according to the displacement extremum, through switching action controlled by a digital signal processing system. Thus the voltage in the piezoelectric patch is enhanced and time shifted in the time domain from the displacement of the vibrating structure. This voltage when shunted through electrical circuit results in increased energy dissipation with enhanced damping effect. This paper proposes to further increase the dissipated energy through a new technique called the synchronized switch damping on negative capacitance and voltage sources (SSDNCV). The idea is to further increase the value of voltage in the piezoelectric patch though the use of negative capacitance and two extra voltage sources in the shunt circuit. First theoretical expressions are derived for SSDNCV method to determine the maximum energy dissipated from the shunt circuit and the corresponding maximum damping. The effectiveness of SSDNCV method, as compared to the previous SSD methods, is then demonstrated in the first resonance mode control of a cantilever beam containing piezoelectric patch. The SSDNCV control reduced the vibration amplitude by 82 % as compared to 63 % and 29 % obtained from SSDNCI and SSDV controls respectively.

Keywords: *Damping, Piezoelectric, Shunt, Switch*

1. Introduction

Vibration control is an important field of studies in engineering, especially the aerospace applications [1-5]. As the aerospace industry progressed, an increased trend has been observed to manufacture structures which are light weight and of larger size. This enables transportation of man and material over long distances at reduced cost [6]. However, such structures need to be vibration controlled at low frequency modes which affect their proper functionality. Recently, piezoelectric (PZT) materials have contributed to overcome problems related to low frequency vibration control of flexible structures. Some of their advantages, as compared to conventional damping materials include small volume, light weight, mechanical simplicity, and ease of integration with the flexible structures. These materials are excellent actuators and sensors with high electromechancial coupling coefficient, which make them ideal for low frequency vibration control applications.

Vibration control using piezoelectric materials can basically be categorized into two main group's *i.e.*, piezoelectric shunt damping (PSD) and active vibration control (AVC).

ISSN: 2005-4297 IJCA
Copyright ⓒ 2015 SERSC

According to Moheimani [7], piezoelectric shunt damping is an alternate to active vibration control. In these techniques, piezoelectric material patches are attached to or embedded into the flexible structures and connected to a network of electrical elements. During operation, the vibration energy is converted into electrical energy by the direct piezoelectric effect. Thus the electrical elements, if properly configured and tuned in a circuit, enables dissipation of the converted electrical energy, thus reducing displacement amplitude of the flexible structure [8-10].

Piezoelectric shunt damping can be further categorized into passive, semi-passive and semi-active techniques. The simplest among these is the passive shunt damping. It consists of shunting the piezoelectric patches with a resistive-inductive RL electrical network [9, 10, 11-14]. Passive shunt damping works effectively for one particular frequency *i.e.*, limited bandwidth. However, if this frequency changes, *e.g.*, due to environmental variations or change of external loads, as observed in actual conditions, this severely affects their control performance. Also, these systems require high shunt impedance values to control low frequency vibration, which is not suitable for onboard aerospace applications. Recently, semi-passive and semi-active shunt damping techniques have been developed in order to effectively overcome the disadvantages of passive damping systems [15-29]. It is pointed out here that there is a difference between semi-passive and semi-active shunt damping techniques, although in literature it has been used interchangeably by different authors to represent different shunt damping circuits with external power supply *e.g.*, Qiu *et al.*, [30]. But, Wang *et al.*, [31], considered an electric shunt circuit which does not provide power to the system as semi-passive, while the rest of the circuits as semi-active.

Over the last decade, synchronized switch damping (SSD), which is a class of semi-passive and semi-active vibration control techniques, have emerged. These techniques are basically nonlinear in nature. Damping of the flexible structure, which is directly proportional to the amount of piezoelectric voltage, is improved by inverting and enhancing the piezoelectric voltage in synchronous with the structure motion. This inverted and enhanced piezoelectric voltage is then dissipated through the network of electrical elements, thus improving the control performance [15-17]. Low frequency vibration attenuation, insensitivity towards resonance frequency variation and enhanced damping performance over a broader bandwidth made these techniques popular among the research community.

Different variations of SSD techniques can be found in literature. The simplest of these is the synchronized switch damping on resistance (SSDS) [15, 16]. In this control technique, the voltage on the piezoelectric patch, which in fact is the image of displacement, is switched to zero when the extremum of displacement is reached. The switching action is performed through a pair of solid state switches driven by a controlled width pulse generated by a simple microcontroller. This process allows piezoelectric voltage magnification and a phase difference appears between piezoelectric strain and the resulting voltage, thus creating energy dissipation. During the switching action, the switch is kept open for most of the time in a period of vibration and is closed only when the extremum of displacement is detected which corresponds to the maximum of strain in the piezoelectric patch. The time for which the switch remains closed is much shorter than the period of vibration. In fact the closed time should be kept as minimum as possible for better electric energy dissipation. In the SSDS technique, the dissipated or the transferred energy E_t during a single frequency vibration period can be written as:

$$E_t = \frac{4\alpha^2}{C_p} u_M^2 \quad , \tag{1}$$

Where α the piezoelectric coefficient or the force factor is, C_p is the blocked capacitance of piezoelectric patch, and u_M is the vibration amplitude [24]. In order to

 Copyright ⓒ 2015 SERSC

quantify the damping performance of a control system, the following performance index A_p in dB is used:

$$A_p = 20\,log(\frac{vibration\ amplitude\ with\ control}{vibration\ amplitude\ without\ control}) . \quad (2)$$

The theoretical value of SSDS for a single vibration mode is given as:

$$A_{SSDS} = 20\,log(\frac{C\omega_o}{C\omega_o+(4\alpha^2/\pi C_p)}) , \quad (3)$$

Where, ω_o is the angular resonance frequency of vibration and C is the mechanical losses coefficient.

Later, Richard [17] improved the control performance of SSDS by including an inductor in the shunt circuit. This technique became known as synchronized switch damping on inductance (SSDI) [18, 22]. A presence of inductance L in the shunt circuit along with the inherent capacitance C_p of piezoelectric material give rise to electrical resonance LC_p circuit. This can be properly tuned to invert and magnify the piezoelectric patch voltage V_p, which is also distorted and time shifted as shown in Figure 1. This increases the energy dissipation from the system and consequently enhances the damping performance. The switch is closed at displacement extrema and is kept closed for half the period of LC_p circuit. The period t_i of the LC_p circuit is chosen to be much smaller than that of the mechanical vibration period and is given by:

$$t_i = \pi\sqrt{LC_p} . \quad (4)$$

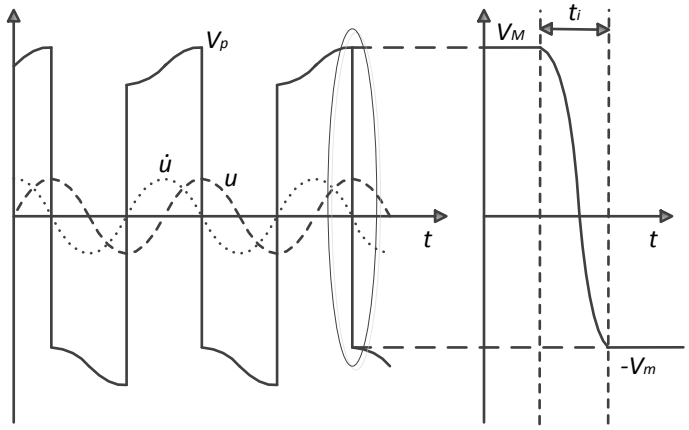

Figure 1. Piezoelectric Patch Voltage and the Structural Displacement

The dissipated energy during a single frequency vibration period in SSDI technique is given by:

$$E_t = \frac{4\alpha^2}{C_p}\frac{1+\gamma}{1-\gamma}u_M^2 , \quad (5)$$

Where γ is the voltage inversion coefficient? A comparison of equation (5) with equation (1) shows that the transferred energy is magnified [24]. The theoretical value of SSDI for a single vibration mode is given as:

$$A_{SSDI} = 20\,log(\frac{C\omega_o}{C\omega_o+(4\alpha^2/\pi C_p)(1+\gamma)/1-\gamma)}) . \quad (6)$$

In pursuit of generating higher piezoelectric patch voltage which is directly related to higher damping performance, Lefeuvre *et al.*, [23] added two voltage sources, in series with the inductor in the shunt circuit of SSDI. This technique is called synchronized switch damping on voltage sources (SSDV) [24, 35]. The addition of two voltage sources

Copyright ⓒ 2015 SERSC

further increased the inverted voltage magnitude of piezoelectric materials, thus increasing the energy dissipation and enhancing the damping performance as compared to previous SSD techniques. The dissipated energy during a single frequency vibration period in SSDV technique is given by:

$$E_t = (\frac{4\alpha^2}{C_p} u_M^2 + 4\alpha u_M V_{cc}) \frac{1+\gamma}{1-\gamma} \ , \quad (7)$$

Where V_{cc} is the additional constant voltage source in the shunt circuit. Equation (7) clearly shows further improvement in the transferred energy as compared to the SSDI technique. The theoretical value of SSDV for a single vibration mode is given as:

$$A_{SSDV} = 20\, log(\frac{C\omega_o}{C\omega_o + (4\alpha^2/\pi C_p)(1+\gamma)/(1-\gamma)} \times (1 - \frac{4}{\pi}\frac{1+\gamma}{1-\gamma}\frac{\alpha V_{cc}}{F_M})) \ . \quad (8)$$

Recently, Ji *et al.*, [32] proposed to replace inductor with a negative capacitor in the shunt circuit of SSDI. This new technique is called synchronized switch damping on negative capacitance (SSDNC). As the magnitude of voltage on the piezoelectric patch depends upon the quality factor of the inductor or the quality factor of the circuit [18, 22], it was found that inductors wound from wire have low quality factors which could not be increased substantially. However, even in the absence of inductor and consequently the electrical resonance in the shunt circuit, voltage inversion is still possible as the whole circuit becomes capacitive in the SSDNC technique. The magnitude of piezoelectric patch voltage depends upon the ratio of piezoelectric patch inherent capacitance C_p and the negative capacitance $-C_n$. Thus by choosing an appropriate negative capacitance value, piezoelectric patch voltage can be amplified which in turn enhances the damping performance. The dissipated energy during a single frequency vibration period in SSDNC technique is given by:

$$E_t = \frac{C_n}{C_n - C_p}\frac{4\alpha^2}{C_p} u_M^2. \quad (9)$$

The theoretical value of SSDNC for a single vibration mode is given as:

$$A_{SSDNC} = 20\, log(\frac{C\omega_o}{C\omega_o + (4\alpha^2/\pi C_p)(C_n/C_n - C_p)}) \quad . \quad (10)$$

Some researchers have tried to combine both the resonant nature of SSDI technique and capacitive nature of SSDNC technique into a new technique called synchronized switch damping on negative capacitance and inductance (SSDNCI) *e.g.*, Mokrani *et al.*, [33]. They identified that in the SSDNC technique, the negative capacitor saturated due to the high current generated during the closing of switch. This problem was effectively solved by using an inductor along with the negative capacitor in the shunt circuit. The inductor limited the amount of current supplied by the negative capacitor, thus improving the damping performance in relation to SSDNC technique. Recently, Han *et al.*, [34] proposed an updated version of SSDNCI technique. The authors argued that in SSDNCI technique, the piezoelectric patch is never held in isolation, contrary to SSDI technique. In fact the negative capacitance is involved during both open and close switch states in the SSDNCI technique. In SSDI technique, the voltage inversion ratio during the close switch state, mainly determines the piezoelectric patch voltage magnitude [25]. However, the intrinsic resistance of the shunt components limits the magnitude of the inversion ratio. In the SSDNCI technique, the negative capacitance enhanced the damping performance in both switching states. The dissipated energy in SSDNCI increased by $(1+\delta)^{-3/2}$ in comparison with SSDI, where δ is the ratio between the negative capacitance and inherent piezoelectric patch capacitance.

This paper proposes a new technique called synchronized switch damping on negative capacitance and voltage sources (SSDNCV). The idea is to further increase the magnitude of voltage on the piezoelectric patch by inducing external voltage into the shunt circuit of

 Copyright ⓒ 2015 SERSC

SSDNCI. First theoretical analysis of SSDNCV is presented to determine the maximum amount of energy dissipated from the shunt circuit and the corresponding maximum damping. Then experiments are performed for the vibration control of an aluminum cantilever beam containing piezoelectric patch. The results are then discussed and compared to the previous SSD techniques for the control of first frequency mode in order to determine better damping performance of the proposed technique. The paper is closed by presenting conclusion and suggestion for future direction.

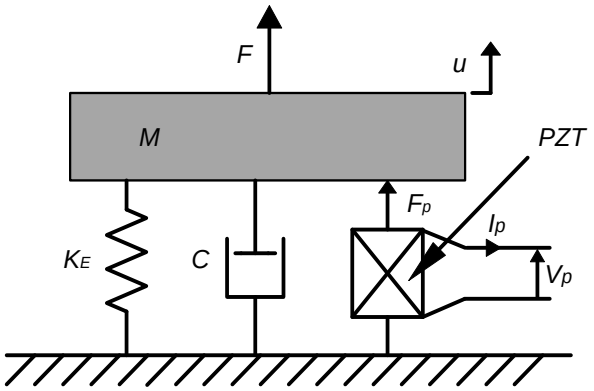

Figure 2. Schematic Representation of the Electromechanical Model for Piezoelectric Shunt Damping. PZT: Piezoelectric Patch

2. Theoretical Analysis

2.1. Dynamic Modeling of Piezostructural System

The electromechanical behavior of a vibrating structure containing piezoelectric patch, also called piezostructure, can be modeled as a spring-mass-damper system as shown in Figure 2. In its simplest form, the structure can be modeled as a second order model if it is driven around one of its resonance frequencies under harmonic excitation [24]. Assuming linear elastic properties for the structure and the piezoelectric patch, differential equation (11) can be established:

$$M\ddot{u} + C\dot{u} + K_E u = \sum F_i \,, \tag{11}$$

where M represents the equivalent rigid mass and C is the mechanical losses coefficient, K_E is the equivalent stiffness of the mechanical structure and piezoelectric patch in a short-circuited condition, u is the rigid mass displacement and $\sum F_i$ represent the sum of all other forces applied to equivalent rigid mass including forces applied by the piezoelectric patch.

Equations (12) and (13) describe the electromechanical coupling of piezoelectric patch bonded on the vibrating structure:

$$F_p = -\alpha V_p \quad , \tag{12}$$

$$I_p = \alpha\dot{u} - C_p\dot{V}_p \quad , \tag{13}$$

Where F_p is the electrically dependent part of the force applied by the piezoelectric patch on the structure, α is the force factor, C_p is the blocked capacitance of piezoelectric patch and I_p is the outgoing current from piezoelectric patch. M, K_E, α and C_p can be determined from the structure and piezoelectric patch characteristics and geometry. As $\sum F_i$ is the combination of F_p and the external applied force on the structure i.e. the excitation force F, therefore equation (11) can be written as:

Copyright ⓒ 2015 SERSC

$$M\ddot{u} + C\dot{u} + K_E u = F - \alpha V_p \ , \quad (14)$$

Which represents the differential equation of motion of the electromechanical vibration system.

Multiplying both sides of equation (14) by velocity and integrating over the time variable gives us the following energy equation (15):

$$\int F\dot{u}\, dt = \frac{1}{2}M\dot{u}^2 + \frac{1}{2}K_E u^2 + \int C\dot{u}^2\, dt + \int \alpha V_p \dot{u}\ dt \ , \quad (15)$$

Which represents the provided energy in terms of kinetic energy, potential energy, mechanical losses and transferred energy. Here the transferred energy represents conversion of a part of mechanical energy to electrical energy. By maximizing this energy, the mechanical energy corresponding to kinetic and potential energy in the structure can be minimized [24].

2.2. Damping Performance Of SSDNCV Technique

The new technique proposed in this paper, called the synchronized switch damping on negative capacitance and voltage sources (SSDNCV), combines the effect of both SSDV and SSDNC in order to further increase the voltage of piezoelectric patch for enhanced damping performance. Voltage inversion on the piezoelectric patch takes place via the capacitance transient charging (in SSDNC) and circuit oscillation due to a LC_p resonance (in SSDV). The schematic diagram of SSDNCV technique is shown in Figure 3. It shows two additional constant voltage sources V_{cc} and two switches i.e. $Switch\ 1$ and $Switch\ 2$, in series with other shunt circuit components. The role of the additional voltage sources is to further increase the voltage on the piezoelectric patch in comparison with SSDNCI, thus increasing the damping performance.

Figure 4 shows the theoretical waveforms of piezoelectric patch voltage and the structural displacement during the switching process under steady state conditions. $Switch\ 1$ is closed when maximum of strain or displacement occurs, which corresponds to the maximum piezoelectric patch voltage, and remains closed for the time period t_i. The magnitude of piezoelectric patch voltages before and after the switching action are assumed to be V_M and V_m respectively. $Switch\ 2$ works in a symmetrical way to $Switch\ 1$ and is closed when the minimum of strain or displacement occurs, which corresponds to the minimum of piezoelectric patch voltage and is opened after a closing time period t_i.

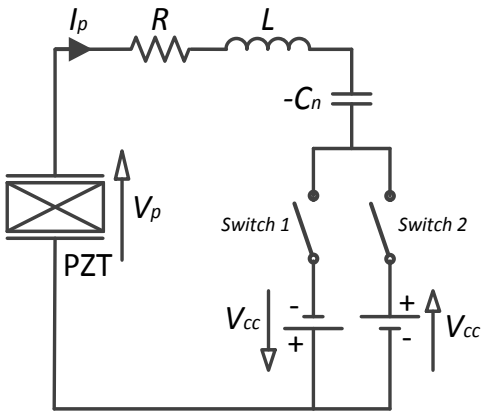

Figure 3. Schematic Diagram of SSDNCV PZT: Piezoelectric Patch

 Copyright ⓒ 2015 SERSC

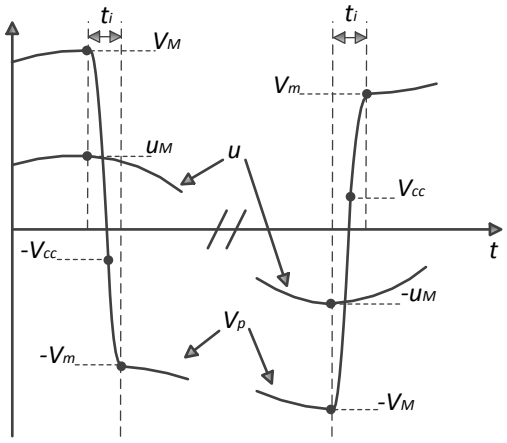

Figure 4. Voltage on the Piezoelectric Patch and the Structural Displacement [24]

Considering half a period of mechanical vibration which corresponds to two voltage inversion cycles, the relationship between V_M and V_m can be expressed as [24]:

$$V_M = V_m + \frac{2\alpha}{C_p} u_M \tag{16}$$

The last term on the right side of equation (15), which corresponds to the transferred energy, can be written as the following integral function of voltage V_p and displacement u [24]:

$$\int \alpha V_p \dot{u}\ dt = \int \alpha V_p\ du\ . \tag{17}$$

The transferred energy during the whole process can be represented by an energy cycle as shown in Figure 5, under the condition that the structure motion is periodic. The transferred energy E_t during the period is given by equation (18):

$$E_t = \int_{period} \alpha V_p\ du = 2\alpha u_M (V_m + V_M)\ . \tag{18}$$

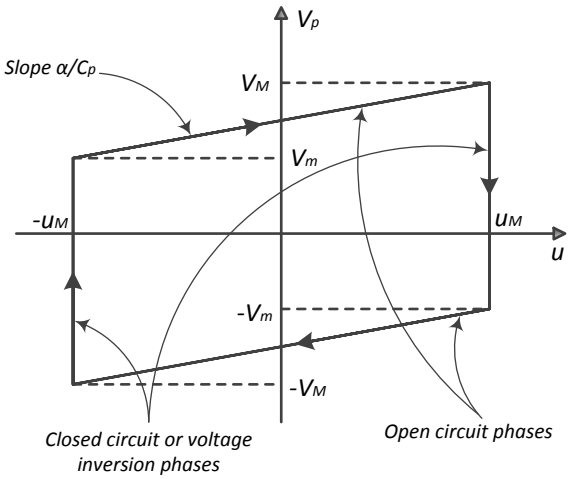

Figure 5. Energy Cycle Showing Open and Closed Circuit Phases [24]

The voltage inversion across the voltage source V_{cc} can be expressed as [24]:

$$V_m - V_{cc} = \gamma (V_M + V_{cc})\ . \tag{19}$$

Copyright ⓒ 2015 SERSC

In case of SSDNC [32], the magnitude of voltage on the piezoelectric patch after switching is expressed as:

$$V_m = \frac{C_p}{C_n - C_p}\frac{\alpha}{C_p}u_M \quad , \tag{20}$$

While the total voltage on the piezoelectric patch before and after the switching is given as:

$$V_M + V_m = \frac{C_n}{C_n - C_p}\frac{2\alpha}{C_p}u_M \ . \tag{21}$$

Putting equations (20) and (21) in equation (19) gives us the expression of voltage inversion in SSDNCV as:

$$\frac{C_p}{C_n - C_p}\frac{\alpha}{C_p}u_M - V_{cc} = \gamma[(\frac{2C_n - C_p}{C_n - C_p})\frac{\alpha}{C_p}u_M + V_{cc}] \ . \tag{22}$$

Assuming resonance frequency excitation and $\pi/2$ phase difference of displacement behind the excitation force, from equation (15) we can write the work done by the excitation force and energy consumed in the mechanical damping, under open-circuited condition, as [32]:

$$\int_0^T F\dot{u}\, dt = \pi F_M u_M \quad \text{and} \tag{23}$$

$$\int_0^T C\dot{u}^2\, dt = \pi C\omega_o u_M^2 \ , \tag{24}$$

Where F_M is the force of excitation, C is the mechanical losses coefficient and ω_o is the resonance frequency of vibration. As under the open-circuited condition, the piezoelectric patch is not connected to the shunt circuit, therefore there is no energy dissipation. Thus equation (23) and (24) should be equal. Hence, the vibration amplitude in the uncontrolled condition can be written as:

$$u_{M(without\ control)} = \frac{F_M}{C\omega_o} \quad , \tag{25}$$

The dissipated or the transferred during a period of vibration for SSDNCV can be easily calculated from the energy cycle shown in Figure 5 [24] and expressed as follows:

$$E_t = (\frac{4\alpha^2}{C_p}u_M^2 + 4\alpha u_M V_{cc})(\frac{1+\gamma}{1-\gamma})(\frac{C_n}{C_n - C_p}) \ . \tag{26}$$

Equation (26) shows an increase in the dissipated energy as compared to the previous SSD techniques as the energy cycle increases along the voltage axis in Figure 5.

In the closed circuit condition, the work done by the force of excitation on the piezostructure should be balanced out by the corresponding energy dissipation by the mechanical damping and the piezoelectric patch [32]. In this respect, the vibration amplitude under controlled condition can be written as:

$$u_{M(with\ control)} = \frac{F_M(4/\pi)[\frac{(1+\gamma)}{(1-\gamma)}\frac{C_n}{(C_n - C_p)}]\alpha V_{cc}}{C\omega_o + (4\alpha^2/\pi C_p)\frac{(1+\gamma)}{(1-\gamma)}\frac{C_n}{(C_n - C_p)}} \ . \tag{27}$$

From equations (25) and (27) and using equation (2), the theoretical value of damping performance of SSDNCV can be expressed as:

$$A_{SSDNCV} = 20\, log(\frac{C\omega_o}{C\omega_o + (4\alpha^2/\pi C_p)\frac{(1+\gamma)}{(1-\gamma)}\frac{C_n}{(C_n - C_p)}} \times (1 - \frac{4}{\pi}\frac{(1+\gamma)}{(1-\gamma)}\frac{C_n}{(C_n - C_p)}\frac{\alpha V_{cc}}{F_M})). \tag{28}$$

Equation (28) shows that better damping performance can be achieved by keeping the absolute value of A_{SSDNCV} larger.

 Copyright ⓒ 2015 SERSC

3. Experimental Setup and Control Scheme

The complete experimental setup is shown in Figure 6. It consists of an aluminum cantilever beam clamped at one end to an electromagnetic exciter which generates a periodic force. Two piezoelectric patches are used during the experiments. One patch is bonded on the top surface of the cantilever beam and is used as an actuator for control purpose. The other patch is bonded on the bottom surface of the cantilever beam and is used as a displacement sensor. The leftmost edge of both the piezoelectric patches is at a distance of 10 mm from the clamped end of the beam. The poling direction of the piezoelectric patches is perpendicular to the beam while electromagnetic coupling coefficient k_{31} mainly drives the piezoelectric response. The electronic switch is driven by a DSP environment based on a National Instruments PCIe-7842R RIO device using Labview software. The electronic switch is turned by a trigger signal generated at the point of displacement extremum so that voltage on the piezoelectric control patch is inverted. The trigger signal is generated by the DSP system according to the following equation [36]:

$$(V_0 - V_1)(V_1 - V_2) < 0\,, \tag{29}$$

Where V_0, V_1 and V_2 are the voltages from the sensor at three consecutive sampling points t_0 , t_1 and t_2 respectively. As voltage from the sensor corresponds to the displacement of the cantilever beam, therefore maximum or minimum displacement is detected at t_1 by the DSP system when equation (29) is satisfied. The material properties and dimensions of the aluminum beam and piezoelectric patches are summarized in Table 1.

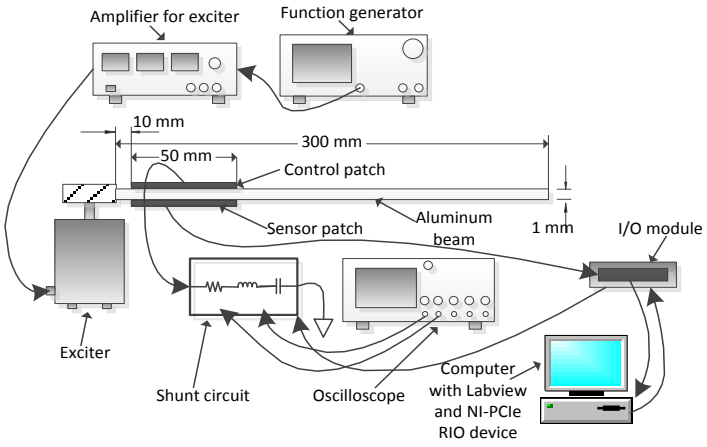

Figure 6. Experimental Setup

Table 1. Aluminum Beam and Piezoelectric Patches Properties and Dimensions

Aluminum beam	Size	300 x 40 x 1 mm
	Elastic modulus	E_b = 70 GPa
	Mass density	ρ_b = 2700 kg/m^3
Piezoelectric patches	Size	50 x 40 x 0.5 mm
	Elastic modulus	E_p = 66 GPa
	Mass density	ρ_p = 7450 kg/m^3
	Electromechanical coupling coefficient	k_{31} = 0.36
	Free capacitance	C_p = 67 nF

Copyright ⓒ 2015 SERSC

A negative capacitance shunt can only be realized by a negative impedance converter and is schematically represented in Figure 7 [37]. It is an active storage element due to the use of an operational amplifier in combination with passive elements. The circuit's input impedance can be written as:

$$Z_{in} = -\frac{1}{sR_2C_g/R_1} = -\frac{1}{sC_n} \quad (30)$$

Where $-C_n = -R_2C_g/R_1$ gives us the negative capacitance. Thus a particular negative capacitance can be produced by varying the values of R_1,R_2 or C_g. In our experiments, the values of R_1,R_2 and C_g were 5.0 kΩ, 6.73 kΩ and 52 nF respectively. This gave us the value of negative capacitance equal to -70 nF. The value of inductor and resistor used during the experiments is 1.08 H and 1KΩ respectively. The quality factor Q_i [23] of the circuit is 4.01 and the voltage inversion coefficient γ [24] is 0.67.

4. Results and Discussion

For comparison purpose, experiments are performed without control, with SSDV technique, SSDNCI technique and SSDNCV technique for the control of vibration at the first resonance frequency of the cantilever beam around 9.5 Hz. The cantilever beam was excited at its first resonance frequency and the amplitude of uncontrolled vibration was set at 6.6 mm which is equivalent to -43.6 dB (decibel).

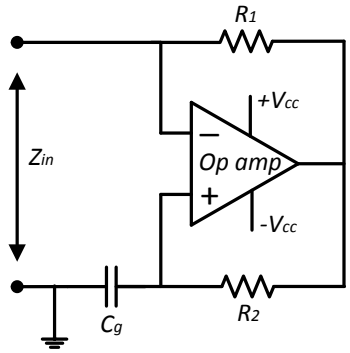

Figure 7. Negative Capacitance Circuit Schematic

4.1. Damping Performance of SSDV Technique

In this section we investigate that how the damping performance of SSDV is affected by the variation of voltage source V_{cc}. Figure 8 shows the effect of variation of voltage source on the displacement amplitude of beam for the control of first resonance mode. Without control the displacement amplitude is -43.6 dB. When the value of V_{cc} is increased, the displacement amplitude is decreased. This trend is observed until the value of V_{cc} is equal to 3.4 V, for which the value of displacement amplitude is -46.5 dB. When the voltage is further increased, the displacement amplitude starts to increase again. Thus the optimal voltage is 3.4 V for which the minimum displacement amplitude is observed for the control of first resonance mode of the piezostructure. If the value of voltage is too large then it destabilizes the system.

Figure 9 shows the time response of displacement at the optimal voltage of 3.4 V using the SSDV technique. The amplitude of displacement is reduced to 4.7 mm from 6.6 mm as observed for the uncontrolled state. This corresponds to 29 % of amplitude reduction using SSDV technique. The percent reduction is not too large and it is attributed to the lower values of electromechanical coupling coefficient and free capacitance of

 Copyright ⓒ 2015 SERSC

piezoelectric patch used for control purpose. Using piezoelectric materials with better properties may further improve the SSDV performance.

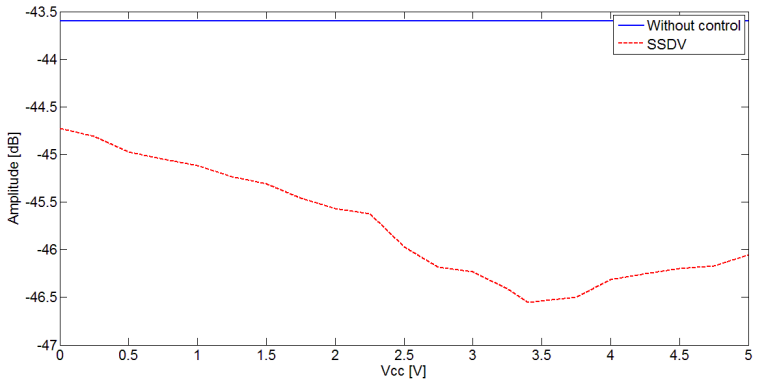

Figure 8. Variation of Vibration Amplitude through SSDV Technique for the Control of First Mode

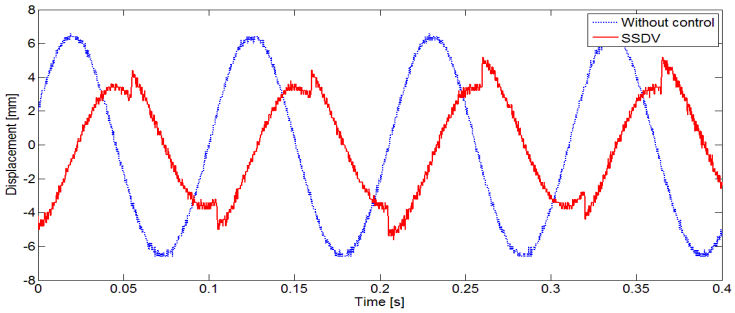

Figure 9. Time Response of Displacement through SSDV Technique at $V_{cc} = 3.4$ V

The irregular sinusoidal waveform can be attributed to the sharp edges of piezoelectric voltage generated by the sensor piezoelectric patch. As the control piezoelectric patch and the sensor piezoelectric patch are bonded on the aluminum beam, so their negative connections are common. Thus during the experiment, voltage from the sensor piezoelectric patch affects the output voltage of the control piezoelectric patch. Another contributing factor may be due to the high current generated during the switching process which affects the displacement amplitude of the piezostructure. Figure 10 shows the corresponding voltage and displacement waveforms for the control of first resonance mode through SSDV technique. Figure 10 also shows the piezoelectric patch voltage in the uncontrolled state which is equal to 6.6 V. Thus after the application of SSDV technique the piezoelectric patch voltage is inverted and increased to 8.2 V. Thus the dissipated energy, which depends upon the magnitude of voltage on the piezoelectric patch, is enhanced and the damping effect is increased.

Copyright ⓒ 2015 SERSC

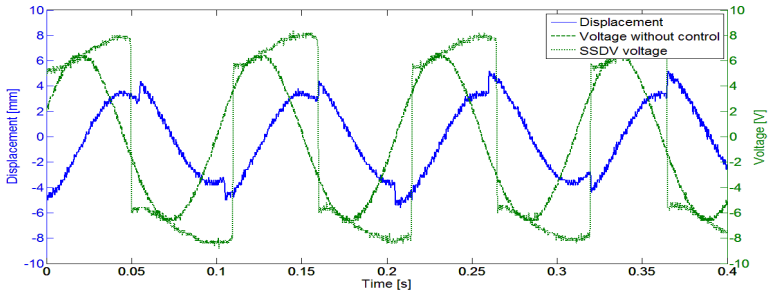

Figure 10. Voltage and Displacement Waveforms for the Control of First Mode through SSDV Technique ($V_{cc} = 3.4$ V)

4.2. Damping Performance of SSDNCV Technique

In this section we investigate how the damping performance of SSDNCV is affected by the variation of V_{cc} and $-C_n$. Figures 11 (a) and (b) shows the variation of vibration amplitude at constant negative capacitance and constant voltage sources respectively for the control of first resonance frequency of the piezostructure. When the value of V_{cc} is 0 V, SSDNCV system is the same as SSDNCI system. When the SSDNCI system is used for control purpose, the displacement amplitude is reduced to 2.4 mm as shown in Figure 14, which is equivalent to -52.4 dB. Thus a reduction of 63 % in displacement amplitude is observed by using the SSDNCI technique. This percent reduction in displacement is due to further voltage magnification of piezoelectric patch as compared to the SSDV technique. The value of magnified piezoelectric patch voltage is equal to 9.8 V as shown in Figure 15.

During repeated experiments using the SSDNCV technique, the optimal values of V_{cc} and$-C_n$, for which the best damping performance is achieved, were found to be 4.7 V and -70 nF respectively. From Figure 11(a) it is clear that as the voltage V_{cc} is increased, the vibration amplitude is decreased until the value of V_{cc} equal to 4.7 V is reached. A further increase in voltage after this value increases the vibration amplitude. If the voltage is increased too much, then the system becomes unstable. Figure 11(b) shows how the value of negative capacitance $-C_n$ affects the control performance of SSDNCV system. From the experiments it was found that keeping the value of negative capacitance closer to the inherent capacitance of piezoelectric patch gives better damping performance. In fact optimal damping performance is achieved by keeping the value of negative capacitance slightly greater than the inherent capacitance of the piezoelectric patch as shown in Figure 11(b). A value of negative capacitance too less or too greater than the piezoelectric patch capacitance destabilizes the system. In fact from the experiments it was observed that the vibration amplitude increases beyond the displacement amplitude for the uncontrolled case for too high or too low negative capacitance values. Furthermore, it is also observed that values of negative capacitance which are lower than the inherent capacitance of the piezoelectric patch have more profound effect on the destabilization of the piezostructure than the values which are higher.

Figure 12 shows the time response of the displacement for the control of first resonance mode using the SSDNCV technique at $V_{cc} = 4.7$ V and $-C_n = -70$ nF. The displacement amplitude is reduced to 1.2 mm which is equivalent to -58.41 dB. Thus the vibration amplitude is reduced by 82 % by using the SSDNCV system as compared to 63 % and 29 % as observed in SSDNCI and SSDV systems respectively. This increased damping performance is attributed to fact that larger voltage magnification is achieved in the SSDNCV system as compared to the SSDNCI and SSDV systems. In fact the piezoelectric patch voltage is increased to 14.5 V as shown in Figure 13. The control performance of SSDNCV also has a positive effect on the shape of the sinusoidal waveform of the displacement. This can be attributed to the fact that in the SSDNCV

 Copyright ⓒ 2015 SERSC

technique the displacement is much lower than the SSDNCI and SSDV techniques. This results in a low piezoelectric sensor voltage output for the corresponding displacement of 1.2 mm. Thus voltages from the piezoelectric sensor do not have much effect on the piezoelectric control patch voltages. This results in a smoother displacement sinusoidal waveform when SSDNCV system is in operation.

In order to compare the control performances of different SSD techniques as discussed above, the spectrums of normalized displacements in decibels of the first resonance mode with uncontrolled displacement, the displacement with SSDV control, SSDNCI control and SSDNCV control is obtained as shown in Figure 16 (a). In the spectrum of uncontrolled displacement, small peaks can be found at high order harmonic frequencies of the first resonance mode. This can be attributed to the fact that the system is nonlinear in nature. The spectrums of displacements are magnified around the first resonance frequency of 9.5 Hz in order to clearly identify the amount of reduction in displacement amplitudes as shown in Figure 16 (b). From these plots it is clear that SSDV control reduces the first mode by only -2.95 dB, while for the SSDNCI and SSDNCV controls this reduction was equal to -8.87 dB and -14.81 dB respectively. The large difference in values between reduction through SSDV control and SSDNCI / SSDNCV controls is due to the fact that for the SSDNCI and SSDNCV controls the negative capacitance in the shunt circuit artificially increases the electromechancial coupling coefficient [9, 38] which in turn increases the damping performance. The control performances of SSDV control, SSDNCI control and SSDNCV control is summarized in Table 2.

5. Conclusion

This paper proposed a new SSD technique which enhanced the damping effectiveness of SSDV and SSDNCI control. The dissipated energy is indeed increased by adding voltage sources in the switching shunt circuit of SSDV control. This dissipated energy is further increased when external voltages are applied to the SSD shunt circuit consisting of negative capacitance and inductance. This give rise to the proposed new technique herein called the synchronized switch damping on negative capacitance and voltage sources (SSDNCV). It has been shown in the SSDNCV control that magnitude of voltage on the piezoelectric patch, which is directly related to the amount of energy dissipation, depends upon the value of negative capacitance used in the shunt circuit. This value should be kept near to the inherent capacitance of the piezoelectric patch. In fact it is found that the value of negative capacitance slightly greater than the piezoelectric patch capacitance gives optimal damping performance. Experiments are performed on an aluminum cantilever beam consisting of piezoelectric patches. The damping performance of SSDNCV method is then compared to SSDV method and SSDNCI method for the first resonance mode control of the cantilever beam. The effect of variation of negative capacitance and voltage sources on the damping performance of SSDNCV method is also investigated. From these results, the optimal values of negative capacitance and voltage sources are found which give the best damping results. The experimental results show that SSDNCV method give better control results as compared to SSDV and SSDNCI methods. The displacement amplitude reduction of 82 % is observed for the SSDNCV method as compared to 63 % and 29 % for SSDNCI and SSDV methods respectively.

The two external voltage supplies in SSDNCV control may appear to be a drawback of this method. However, this can be possibly overcome by generating these voltages from the structure motion using energy harvesting techniques. Another point which needs to be addressed for further improvement in performance of SSDNCV method is the adaptive adjustment of the voltage sources. When the vibration level is low, the constant voltage sources in the shunt circuit may actually excite the structure instead of controlling it. Thus adaptive adjustment of voltage sources according to the amplitude of vibration may give better damping results not only for first mode control but also for broadband control.

Copyright ⓒ 2015 SERSC

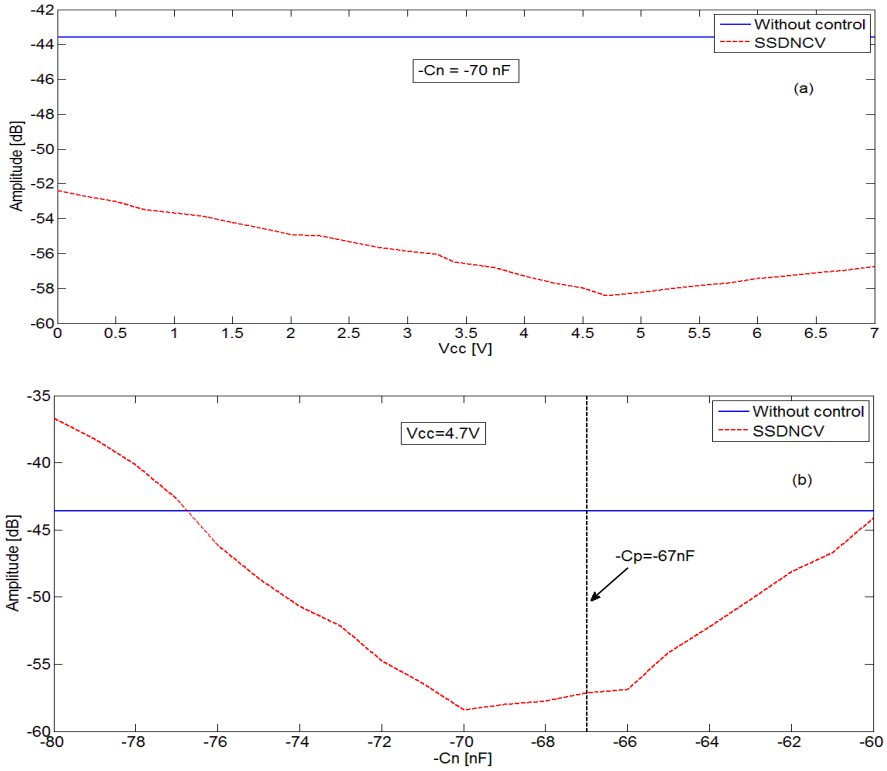

Figure 11. Variation of Vibration Amplitude through SSDNCV Technique for the Control of First Mode at: (A)$-C_n = -70$ nF, (B) $V_{cc} = 4.7$ V

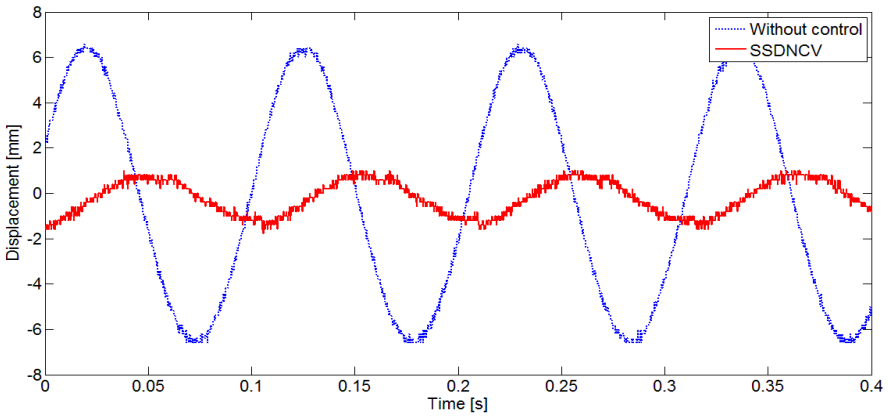

Figure 12. Time Response of Displacement through SSDNCV Technique at $V_{cc} = 4.7$ V and $-C_n = -70$ nF

Copyright ⓒ 2015 SERSC

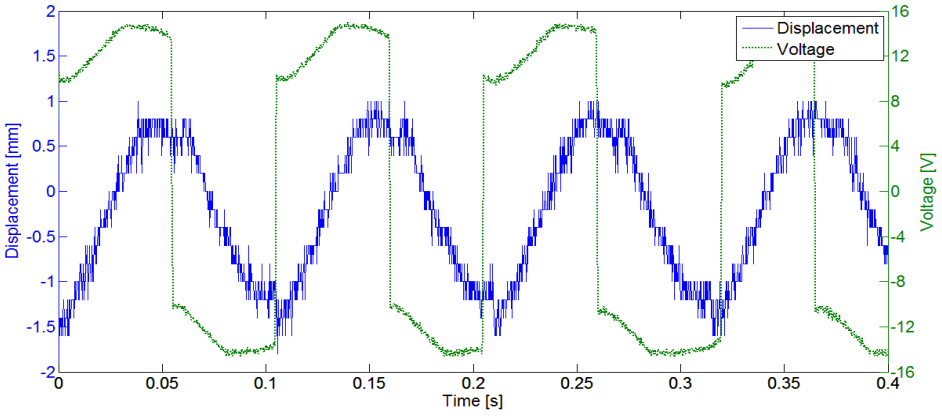

Figure 13. Voltage and Displacement Waveforms for the Control of First Mode through SSDNCV Technique at $V_{cc} = 4.7$ V And $-C_n = -70$ nF

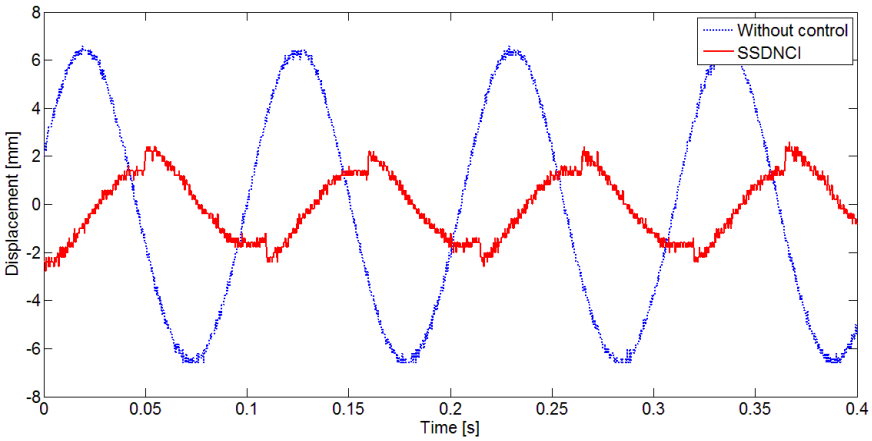

Figure 14. Time Response of Displacement through SSDNCI Technique At $-C_n = -70$nF

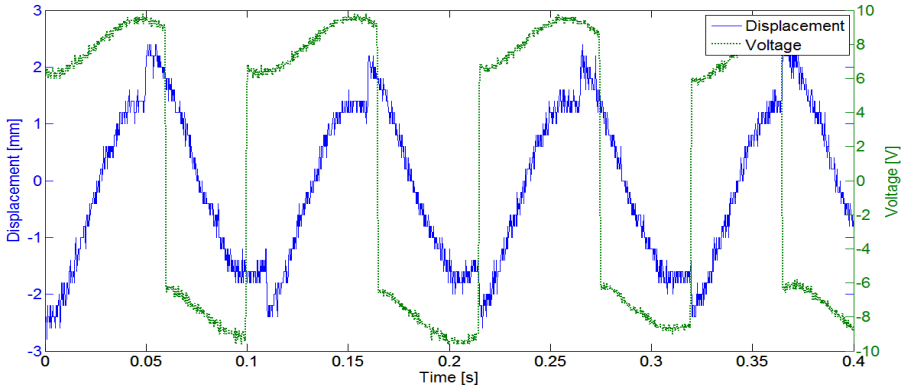

Figure 15. Voltage and Displacement Waveforms for the Control of First Mode through SSDNCI Technique At$-C_n = -70$ nF

Copyright ⓒ 2015 SERSC

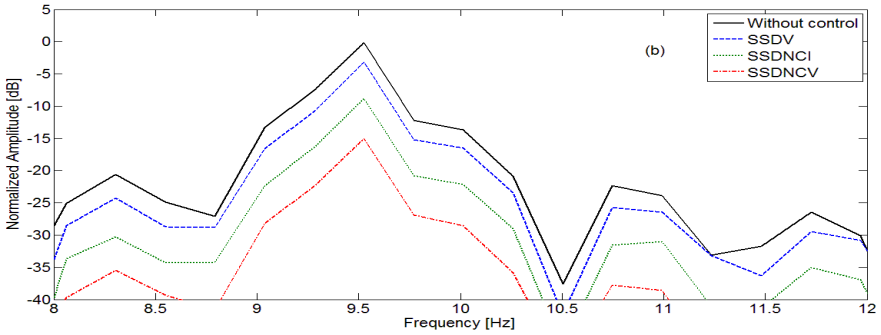

Figure 16. The Spectrums of Normalized Displacements of the First Resonance Mode through SSDV, SSDNCI and SSDNCV Techniques: (A) Actual, (B) Magnified Around 9.5 Hz

Table 2. The Control Performance of SSDV, SSDNCI and SSDNCV in First Resonance Mode Control

Amplitude without control (dB)	Amplitude with SSDV control (dB)	Attenuation with SSDV control (dB)	Amplitude with SSDNCI control (dB)	Attenuation with SSDNCI control (dB)	Amplitude with SSDNCV control (dB)	Attenuation with SSDNCV control (dB)
-0.22	-3.17	-2.95	-9.09	-8.87	-15.03	-14.81

Acknowledgements

This work was sponsored by Qing Lan Project and a Project funded by the PAPD. The authors are also grateful to the Fundamental Research Funds for the Central Universities (No. NS2013010).

References

[1] M. A. Hopkins, D. A. Henderson, R. W. Moses, T. Ryall, D. G. Zimcik and R. L. Spangler, "Active vibration suppression systems applied to twin-tail buffering", Proc. SPIE Smart Structures and Materials: Industrial and Commercial Application of Smart Structures Technologies, DOI:10.1117/12.310663, vol. 3326, **(1998)**, pp. 27-33.
[2] J. Simpson and J. Schweiger, "Industrial approach to piezoelectric damping of large fighter aircraft components", Proc. SPIE Smart Structures and Materials: Industrial and Commercial Application of Smart Structures Technologies, DOI:10.1117/12.310669, vol. 3326, **(1998)**, pp. 34-46.
[3] S. Kim, C. Han and C. Yun, "Improvement of aeroelastic stability of hingeless helicopter rotor blade by passive piezoelectric damping", Proc. SPIE Smart Structures and Materials: Passive Damping and Isolation, DOI:10.1117/12.349776, vol. 3672, **(1999)**, pp. 131-141.
[4] S. Wu, T. L. Turner and S. A. Rizzi, "Piezoelectric shunt vibration damping of an F-15 panel under high-acoustic excitation", Proc. SPIE Smart Structures and Materials: Damping and Isolation, DOI:10.1117/12.384568, vol. 3989, **(2000)**, pp. 276-287.
[5] E. F. Sheta and R. W. Moses, "Active smart material control system for buffet alleviation", Journal of Sound and Vibration, DOI:10.1016/j.jsv.2005.09.002, vol. 292, no. 3-5, **(2006)**, pp. 854–868.
[6] E. M. Qureshi, X. Shen and J. J. Chen, "Vibration control laws via shunted piezoelectric transducers: A review", International Journal of Aeronautical and Space Sciences, DOI:10.5139/IJASS.2014.15.1.1, vol. 15, no. 1, **(2014)**, pp. 1-19.
[7] S. O. R. Moheimani, "A survey of recent innovations in vibration damping and control using shunted piezoelectric transducers", IEEE Transactions on Control Systems Technology, DOI:10.1109/TCST.2003.813371, vol. 11, **(2003)**, pp. 482-494.
[8] C. L. Davis and G. A. Lesieutre, "A modal strain energy approach to the prediction of resistivity shunted piezoceramic damping", Journal of Sound and Vibration, DOI: 10.1006/jsvi.1995.0308, vol. 184, no. 1 , **(1995)**, pp. 129-139.
[9] R. L. Forward, "Electronic damping of vibrations in optical structures", Applied Optics, DOI: 10.1364/AO.18.000690, vol. 18, no. 5, **(1979)**, pp. 690-697.

 Copyright ⓒ 2015 SERSC

[10] N. W. Hagood and A. von Flotow, "Damping of structural vibrations with piezoelectric materials and passive electrical networks", Journal of Sound and Vibration, DOI: 10.1016/0022-460X(91)90762-9, vol. 146, no. 2, **(1991)**, pp. 243-268.
[11] N. W. Hagood and E. F. Crawley, "Experimental investigations of passive enhancement of damping space structures", Journal of Guidance, Control and Dynamics, DOI: 10.2514/3.20763, vol. 14, no. 6, **(1991)**, pp. 1100-1109.
[12] J. J. Hollkamp, "Multimodal passive vibration suppression with piezoelectric materials and resonant shunts", Journal of Intelligent Material Systems and Structures, DOI: 10.1177/1045389X9400500106, vol. 5, no. 1, **(1994)**, pp. 49-56.
[13] H. H. Law, P. L. Rossiter, G. P. Simon and L. L. Koss, "Characterization of mechanical vibration damping by piezoelectric materials", Journal of Sound and Vibration, DOI:10.1006/jsvi.1996.0544, vol. 197, no. 4, **(1996)**, pp. 489-513.
[14] S. Behrens, S. O. R. Moheimani and A. J. Fleming, "Multiple mode current flowing passive piezoelectric shunt controller", Journal of Sound and Vibration, DOI: 10.1016/S0022-460X (02)01380-9, vol. 266, no. 5, **(2003)**, pp. 929-942.
[15] C. Richard, D. Guyomar, D. Audigier and G. Ching, "Semi-passive damping using continuous switching of a piezoelectric device", Proc. SPIE Conf. Passive Damping Isolation, Newport Beach, CA, DOI:10.1117/12.349773, vol. 3672, **(1999)**, pp. 104-111.
[16] W. W. Clark, "Vibration control with state-switched piezoelectric materials", Journal of Intelligent Material Systems and Structures, DOI: 10.1106/18CE-77K4-DYMG-RKBB, vol. 11, no. 4, **(2000)**, pp. 263-271.
[17] C. Richard, D. Guyomar, D. Audigier and H. Bassaler, "Enhanced semi-passive damping using continuous switching of a piezoelectric device on an inductor", Proc. of SPIE Smart Structures and Materials 2000: Damping and Isolation, DOI:10.1117/12.384569, vol. 3989, **(2000)**, pp. 288-299.
[18] D. Guyomar, C. Richard and L. Petit, "Non-linear system for vibration damping", 142nd Meeting of Acoustical Society of America, Fort Lauderdale, FL, **(2001)**.
[19] K. A. Cunefare, "State-switched absorber for vibration control of point-excited beams", Journal of Intelligent Material Systems and Structures, DOI: 10.1177/104538902761402495, vol. 13, no. 2-3, **(2002)**, pp. 97-105.
[20] J. Onoda, K. Makihara and K. Minesugi, "Energy-recycling semi-active method for vibration suppression with piezoelectric transducers", AIAA Journal, DOI: 10.2514/2.2002, vol. 41, no. 4, **(2003)**, pp. 711-719.
[21] L. R. Corr and W. W. Clark, "A novel semi-active multi-modal vibration control law for a piezoceramic actuator", Journal of Vibration and Acoustics, DOI:10.1115/1.1547682, vol. 125, no. 2, **(2003)**, pp. 214-222.
[22] L. Petit, E. Lefeuvre, C. Richard and D. Guyomar, "A broadband semi passive piezoelectric technique for structural damping", Proceedings of SPIE International Symposium on Smart Structure Materials: Damping and Isolation, DOI:10.1117/12.532716, vol. 5386, **(2004)**, pp. 414-425.
[23] E. Lefeuvre, A. Badel, L. Petit, C. Richard and D. Guyomar, "Semi-passive piezoelectric structural damping by synchronized switching on voltage sources", Journal of Intelligent Material Systems and Structures, DOI: 10.1177/1045389X06055810, vol. 17, no. 8-9, **(2006)**, pp. 653-660.
[24] A. Badel, G. Sebald, D. Guyomar and J. Qiu, "Piezoelectric vibration control by synchronized switching on adaptive voltage sources: towards wideband semi-active damping", Journal of the Acoustical Society of America, DOI: 10.1121/1.2184149, vol. 119, no. 5, **(2006)**, pp. 2815-2825.
[25] M. Neubauer and J. Wallaschek, "Analytical and experimental investigation of the frequency ratio and switching law for piezoelectric switching techniques", Smart Materials and Structures, DOI:10.1088/0964-1726/17/3/035003, vol. 17, no. 3, **(2008)**, pp. 035003.
[26] H. Ji, J. Qiu, A. Badel, Y. Chen and K Zhu, "Semi-active vibration control of a composite beam by adaptive synchronized switching on voltage sources based on LMS algorithm", Journal of Intelligent Material Systems and Structures, DOI: 10.1177/1045389X08099967, vol. 20, no. 8, **(2009)**, pp. 939-947.
[27] H. Ji, J. Qiu, K. Zhu, Y. Chen and A. Badel, "Multi-modal vibration control using a synchronized switch based on a displacement switching threshold", Smart Materials and Structures, DOI:10.1088/0964-1726/18/3/035016, vol. 18, no. 3, **(2009)**, pp. 035016.
[28] H. Ji, J. Qiu, K. Zhu and A. Badel, "Two-mode vibration control of a beam using nonlinear synchronized switching damping based on the maximization of converted energy", Journal of Sound and Vibration, DOI:10.1016/j.jsv.2010.01.012, vol. 329, no. 14, **(2010)**, pp. 2751-2767.
[29] H Ji, J. Qiu and P. Xia, "Analysis of energy conversion in two-mode vibration control using synchronized switch damping approach", Journal of Sound and Vibration, DOI: 10.1016/j.jsv.2011.03.004, vol. 330, no. 15, **(2011)**, pp. 3539-3560.
[30] J. Qiu, H. Ji and K. Zhu, "Semi-active vibration control using piezoelectric actuators in smart structures", Frontiers of Mechanical Engineering in China, DOI:10.1007/s11465-009-0068-z, vol. 4, no. 9, **(2009)**, pp. 242–251.
[31] Y. Wang and D. J. Inman, "A survey of control strategies for simultaneous vibration suppression and energy harvesting via piezoceramics", Journal of Intelligent Material Systems and Structures, DOI: 10.1177/1045389X12444485, vol. 23, no. 18, **(2012)**, pp. 2021-2037.

Copyright ⓒ 2015 SERSC

[32] H. Ji, J. Qiu, J. Cheng and D. Inman, "Application of a negative capacitance circuit in synchronized switch damping techniques for vibration suppression", Journal of Vibration and Acoustics, DOI:10.1115/1.4003146, vol. 133, no. 4, **(2011)**, pp. 041015-1-10.
[33] B. Mokrani, G. Rodrigues, B. Ioan, R. Bastaits and A. Preumont, "Synchronized switch damping on inductor and negative capacitance", Journal of Intelligent Material Systems and Structures, DOI: 10.1177/1045389X11433493, vol. 23, no. 18, **(2012)**, pp. 2065-2075.
[34] X. Han, M. Neubauer and J. Wallaschek, "Improved piezoelectric switch shunt damping technique using negative capacitance", Journal of Sound and Vibration, DOI: 10.1016/j.jsv.2012.08.001, vol. 332, no. 1, **(2013)**, pp. 7-16.
[35] A. Faiz, D. Guyomar, L. Petit and C. Buttay, "Wave transmission reduction by a piezoelectric semi-passive technique", Sensors and Actuators, DOI:10.1016/j.sna.2006.02.021, vol. 128, no. 2, **(2006)**, pp. 230–237.
[36] H. Ji, J. Qiu and K. Zhu, "Vibration control of a composite beam using self-sensing semi-active approach", Chinese Journal of Mechanical Engineering, DOI: 10.3901/CJME.2010.0*.***, vol. 23, **(2010)**, pp. 1-8.
[37] P. Horowitz and W. Hill, The Art of Electronics, Cambridge University Press, New York, **(1996)**.
[38] B. De Marneffe and A. Preumont, "Vibration damping with negative capacitance shunts: theory and experiment", Smart Materials and Structures, DOI:10.1088/0964-1726/17/3/035015, vol. 17, no. 3, **(2008)**, pp. 035015.

Authors

Ehtesham Mustafa Qureshi was born in Haripur, Pakistan in 1977. He received the B.Sc. and M.Sc. Mechanical Engineering degrees from N-W.F.P University of Engineering and Technology, Peshawar, Pakistan, in 2000 and 2005, respectively. Currently, he is pursuing the Ph.D. degree in Measuring and Control Technology and Instrumentation from Nanjing University of Aeronautics and Astronautics, China. His research interests include semi-passive, semi-active and self-sensing vibration control of piezoelectric laminated smart structures.

Xing Shen was born in Changzhou, China, in 1975. He is currently a Professor in College of Aerospace Engineering, Nanjing University of Aeronautics and Astronautics, China. He received the Master degree in Material Science and Engineering in 2000 and Ph.D. degree in Measuring and Testing Technologies and Instruments in 2003 from Nanjing University of Aeronautics and Astronautics, China. His research interests are in the field of smart materials and systems: piezoelectric actuators and sensors, actuators design, fabrication, testing and application of smart structures.

Lulu Chang was born in Taizhou, China, in 1992. She received the Bachelor degree in Aircraft Design and Engineering from the College of Aerospace Engineering, Nanjing University of Aeronautics and Astronautics, China in 2014. She is currently pursuing the Ph.D. degree in Measuring and Control Technology and Instrumentation from Nanjing University of Aeronautics and Astronautics, China. Her research interests include smart skins applied in morphing wings and active vibration control of smart structures.

 Copyright ⓒ 2015 SERSC